Used Filter Cartridges as Potential Adsorbents of Organic Pollutants

Martyna Szymańska and Piotr Nowicki *

Department of Applied Chemistry, Faculty of Chemistry, Adam Mickiewicz University in Poznań,
Uniwersytetu Poznańskiego 8, 61-614 Poznań, Poland
* Correspondence: piotrnow@amu.edu.pl

Abstract: The main objective of this study was to assess the usefulness of exhausted activated carbon-based filter cartridges for the removal of organic pollutants from aqueous solutions using the example of two model pollutants: synthetic dyes with different particle sizes, i.e., methylene blue (MB) and malachite green (MG). In order to determine the organic dyes' adsorption mechanism, the effects of phase contact time, initial dye concentration, pH, and temperature of the system were investigated. Langmuir and Freundlich isotherm models were employed to analyze the experimental data. Additionally, all adsorbents were characterized in terms of the ash content, type of porous structure, presence of surface functional groups, pH value, and iodine adsorption number—which is one of the quality control parameters of activated carbons. Adsorption tests have shown that carbonaceous materials from bottle filters and filter jugs can be successfully used for the removal of organic dyes from the liquid phase. The maximum sorption capacity of this type of adsorbent towards methylene blue was 333.06 mg/g, while in the case of malachite green it was 308.75 mg/g. For all carbonaceous materials, a better fit to the experimental data was achieved with a Langmuir isotherm than a Freundlich one. It has also been shown that the efficiency of MB and MG adsorption from aqueous solutions decreases with increasing temperature of the system—the best results were obtained at 25 °C. A better fit of the kinetics data was achieved using the pseudo-second order model.

Keywords: used carbon filters; activated carbons; physicochemical properties; wastewater treatment; adsorption; organic dyes

1. Introduction

Water is the most abundant and fundamental chemical compound on the Earth. About 70% of our planet's surface is covered with water and ice. In turn, as water vapor, it is an essential component of the surrounding atmosphere. Water plays a significant role in nature. For example, it is necessary in photosynthesis or in geochemical processes (i.e., in the weathering of rocks). It also plays a key role in human life. If the human body does not receive the right amount of water, its work may be disturbed, which is why it is so important to constantly supplement it. Consuming adequate amounts of water supports fat burning, the removal of toxins from the body, the absorption of nutrients, and the proper functioning of digestive enzymes [1]. The quality of the water we drink has also a significant impact on the work of our body. Water, as an inseparable part of the ecosystem, is constantly polluted due to human activities. Unfortunately, the processes of its self-purification are not effective enough, which has the consequence of causing partial degradation of the natural environment and a lack of good-quality water all over the world [2]. Consuming water of unknown purity is associated with the risk that many toxic substances can enter the human body and adversely affect our health [3].

Recently, the public's interest in leading a healthy lifestyle has increased. This applies, among others, to the quality of the water we consume. As a result, consumers increasingly demand that the water they use is tasty, clean, and, most importantly, healthy. Unfortunately, the poor condition of the water supply networks means that these requirements are not always met. This problem led to the development of diverse kinds of water filters that

can be easily applied in homes. Jug, bottle, or tap filters are very popular products due to the low cost of their purchase and exploitation [4]. The uncomplicated handling procedure also encourages their use.

One of the main components of filters that plays a significant role in the process of water treatment is activated carbon. It allows to remove many hazardous substances from water, such as pesticides, detergents, aliphatic and aromatic hydrocarbons, phenols and their derivatives, some heavy metal ions, and chemicals that impair the taste and smell of water [5–18], which is why the popularity of water filtration devices based on activated carbon is increasing day by day. However, the use of various types of filter cartridges on a large scale and in the long term leads to the generation of significant amounts of solid waste, for example exhausted ion exchange resins and activated carbons, as well as plastic containers, which require disposal.

Good-quality activated carbon is an expensive product. The cost of replacing the exhausted carbon is quite prohibitive, therefore very often it is regenerated via steam, thermal, chemical, or biological treatment, as well as reused for water filtration or wastewater purification from organic and inorganic impurities [19]. A significant part of the ion exchange resins is also recycled and returned to the material cycle. However, this mainly applies to adsorbents used on an industrial scale or in large household filtering systems. Bottle filters, jug filters, or filter discs (due to the low cost-effectiveness of their transport and regeneration) usually end up in the garbage.

Taking this into account, the main objective of the presented study was to assess the usefulness of utilizing filter cartridges for the removal of synthetic organic dyes from aqueous solutions. Exhausted filter cartridges were separated into parts, and the recovered carbonaceous materials were subjected to adsorption tests against two synthetic dyes of various molecule sizes, i.e., methylene blue and malachite green, which are often used in the textile industry. The influence of the initial concentration of both dyes, pH, and temperature of the system on the efficiency of their removal from the liquid phase was investigated. Additionally, the adsorbents were characterized in terms of the mineral matter content, type of the porous structure, presence of surface functional groups, pH value, and iodine adsorption number.

2. Materials and Methods

2.1. Materials

Activated carbon obtained from the used bottle filter (B, Figure 1a) provided by Dafi (Kielce, Poland) and material from a jug filter (J, Figure 1b) provided by BRITA (Taunusstein, Germany) were used as the starting materials for the presented studies. According to the manufacturer's declaration, the activated carbons included in the filters were obtained by physical activation of coconut shells. After thorough drying at 110 °C, the activated carbons were ground and sieved to a grain size of 0.9 mm and then subjected to physicochemical characterization. Before further investigations, none of the carbonaceous materials had been chemically treated or regenerated (due to economic and environmental aspects).

Figure 1. Exhausted filter cartridges: (**a**) bottle filter and (**b**) jug filter.

2.2. Analytical Procedures

The total ash (mineral matter) content was evaluated by burning the activated carbon samples at 815 °C in a microwave muffle furnace (Phoenix, CEM Corporation, Matthews, IL, USA), according to the procedure described in the national standard ISO 1171:2002.

The textural characterization of the activated carbons was based on the N_2 adsorption-desorption isotherms measured at −196 °C (Autosorb iQ, Quantachrome Instruments, Boynton Beach, FL, USA). Before isotherms measurements, the samples were outgassed under vacuum at temperature of 300 °C. The specific surface area (S_{BET}) of the carbonaceous materials was determined on the basis of the multilayer adsorption Brunner–Emmett–Teller theory in the range of relative pressure (p/p_0) ranging from 0.05 to 0.30. Total pore volume was calculated by converting the N_2 amount adsorbed at p/p_0 ~0.99 to the volume of liquid adsorbate. Pore size distribution was calculated from the adsorption branches of isotherms using the Barrett–Joyner–Halenda (BJH) method. Furthermore, micropore volume and area were determined by the t-plot method.

The acidic–basic nature of the carbon's surface was evaluated according to the Boehm method, described in detail in our previous paper [20]. Volumetric standard of 0.1 mol/dm^3 NaOH (Avantor Performance Materials, Gliwice, Poland) was used to neutralize groups of acidic character, whereas 0.1 mol/dm^3 HCl (Avantor Performance Materials, Gliwice, Poland) was used to neutralize groups of basic nature.

The pH value of activated carbon aqueous extracts was determined using a CP-401 pH-meter equipped with an EPS-1 combination glass electrode, provided by ELMETRON (Zabrze, Poland), according to the procedure described in [21].

The iodine adsorption number of the activated carbon was determined according to the PN-83/C-97555.04 national standard. Briefly: 0.2 g of the activated carbon sample was mixed with 4 cm^3 of 5% hydrochloric acid (Avantor Performance Materials, Gliwice, Poland) and 20 cm^3 of 0.1 mol/dm^3 I_2 solution (Avantor Performance Materials, Gliwice, Poland) and then shaken vigorously for 4 min, filtered through filter paper, and washed with 50 cm^3 of distilled water. The resulting solution was titrated with volumetric standard of 0.1 mol/dm^3 $Na_2S_2O_3$ (Avantor Performance Materials, Gliwice, Poland) in the presence of starch solution as an indicator (Avantor Performance Materials, Gliwice, Poland).

2.3. Adsorption of the Synthetic Organic Dyes

In order to determine the usefulness of the exhausted carbonaceous materials for removal of organic pollutants from the liquid phase, adsorption tests towards methylene blue and malachite green were carried out. These synthetic cationic dyes (representing organic aromatic compounds, Figure 2) are widely used in the textile industry; therefore, significant amounts of them are present in industrial wastewater.

The study of the adsorption abilities of the activated carbon towards methylene blue (MB) and malachite green (MB) was performed according to the following procedure: a series of the activated carbon samples in equal portions of 0.025 g were mixed with 50 cm^3 of the MB and MG aqueous solutions (Avantor Performance Materials, Gliwice, Poland), with the initial concentrations changing in the range of 5 to 200 mg/dm^3, and then the suspensions were stirred magnetically (150 rpm) at 22 ± 1 °C for 12 h to reach the equilibrium state. After that time, the solids were centrifuged at 5000 rpm for 10 min by means of the Frontier ™ centrifuge FC5515, provided by OHAUS (Parsippany, NJ, USA), and then the clear filtrates were collected for spectrophotometric analysis. The MB and MG concentrations in the solution before and after adsorption tests were established using a double-beam UV–Vis spectrophotometer, Cary 100 Bio, provided by Agilent (Santa Clara, CA, USA), at the wavelengths of 664 nm (in the case of methylene blue) and 617 nm (in the case of malachite green), using the previously prepared calibration curves. In order to obtain the calibration curves, solutions with the final concentrations of organic dyes varying in the range of 2.5–15.0 mg/dm^3 were applied. Distilled water was used as a reference sample.
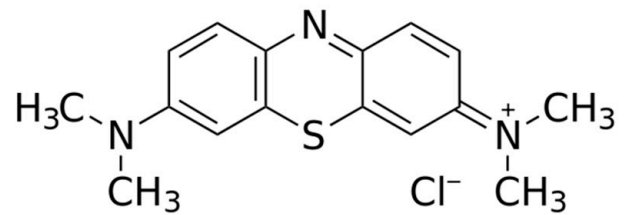
Methylene blue

[7-(dimethylamino)phenothiazin-
3-ylidene]-dimethylazanium;chloride

$C_{16}H_{18}ClN_3S$

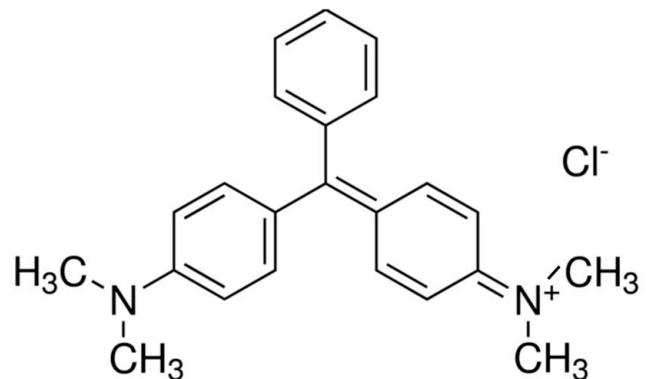M = 319.85 g/mol

λ_{max} = 664 nm

Malachite green
[4-[[4-(dimethylamino)phenyl]-phenylmethylidene]
cyclohexa-2,5-dien-1-ylidene]-dimethylazanium;chloride
$C_{23}H_{25}ClN_2$
M = 364.91 g/mol

λ_{max} = 617 nm

Figure 2. Organic synthetic dyes used during adsorption tests.

The amounts of MB or MG adsorbed at equilibrium state (q_{ads}, mg/g) were calculated from the following Formula (1):

$$q_{ads} = \frac{\Delta c \cdot V_s}{m_{ac}} \tag{1}$$

where: Δc—the difference between starting and final concentration of the MB or MG [mg/dm^3], V_s—the volume of the dye solution [dm^3], and m_{ac}—the mass of activated carbon used for the adsorption test [g].

The effectiveness of methylene blue or malachite green adsorption (Ef_{ads}, %) from the aqueous solutions was calculated according to the following Formula (2):

$$Ef_{ads} = \frac{\Delta c}{c_0} \cdot 100\% \tag{2}$$

where: c_0—the starting concentration of MB or MG [mg/dm^3].

Two adsorption isotherm models were applied to fit the equilibrium data. These isotherms included the Langmuir and Freundlich models, expressed by Equations (3) and (4) [22,23]:

$$q_{eq} = \frac{q_m K_L c_{eq}}{1 + K_L c_{eq}} \tag{3}$$

$$q_{eq} = K_F c_{eq}^{1/n} \tag{4}$$

where: q_{eq}—the equilibrium MB or MG adsorbed amount [mg/g], q_m—the maximal MB or MG adsorbed amount [mg/g], K_L—the Langmuir constant [dm^3/mg], c_{eq}—the equilibrium concentration of MB or MG [mg/dm^3], K_F—the Freundlich constant [mg/g (mg/dm^3)$^{1/n}$], and n—the Freundlich parameter determining the adsorption strength.

The effect of the temperature on the efficiency of adsorption of the above-mentioned organic dyes from the liquid phase was determined according to the following procedure: A portion of 0.025 g of each tested material was placed in flat-bottomed flasks and mixed with 50 cm^3 of the dyes' aqueous solutions. In the case of the activated carbon from bottle

filter (B), the initial MB and MG concentrations were 170 and 160 mg/dm^3, whereas for activated carbon from jug filter (J), they were 150 and 120 mg/dm^3, respectively. Such prepared suspensions were placed on a Unimax 1010 shaker (equipped with an incubator) provided by Heidolph Instruments GmbH & Co. KG (Schwabach, Germany) and shaken for 12 h at temperature of 25, 30, or 35 °C. After shaking, the suspensions were centrifuged, and the final concentrations of MB or MG were determined spectrophotometrically.

The impact of pH on the efficiency of dye adsorption was determined according to the following procedure: A portion of 0.025 g of the activated carbon sample was mixed with 50 cm^3 of MB (c_0 = 170 mg/dm^3) or MG solution (c_0 = 140 mg/dm^3) and shaken vigorously for 12 h at temperature of 25 °C with the pH changing in the range 2.0–12.0. After shaking, the suspension was centrifuged, and the final concentration of organic dyes was determined. The solution pH before the experiments was adjusted by adding appropriate amounts of 0.1 mol/dm^3 HCl or NaOH. The pH was measured using CP-401 pH-meter equipped with EPS-1 combined glass pH electrode.

Kinetic experiments were carried out by contacting 0.025 g of activated carbon with 50 cm^3 of either methylene blue (c_0 = 130 mg/dm^3) or malachite green solution (c_0 = 70 mg/dm^3), at pH 8. The suspension was stirred magnetically (150 rpm) for 6 h, at temperature of 25 °C. The amounts of MB or MG adsorbed by activated carbon after time t (q_t, mg/g) were calculated from the following Formula (5):

$$q_t = \frac{(c_0 - c_t) \cdot V_s}{m_{ac}} \tag{5}$$

where: c_0—the starting concentration of MB or MG [mg/dm^3], c_t—dye concentration at time t [mg/dm^3], V_s—the volume of the dye solution [dm^3], and m_{ac}—the mass of dry activated carbon used for the test [g]. Experimental data were fitted to the pseudo-first order equation (PFO) proposed by Lagergren (Equation (6)) and the pseudo-second order equation (PSO) proposed by Ho and McKay (Equation (7)) [24]:

$$\frac{dq_t}{dt} = k_1 \left(q_{eq} - q_t \right) \tag{6}$$

$$\frac{dq_t}{dt} = k_2 \left(q_{eq} - q_t \right)^2 \tag{7}$$

where: q_{eq}—amount of MB or MG adsorbed in the equilibrium state [mg/g], q_t—the adsorbed amount after time "t" [mg/g], k_1—the pseudo-first order rate constant [1/min], and k_2—the rate constant of the pseudo-second order adsorption [g/(mg·min)].
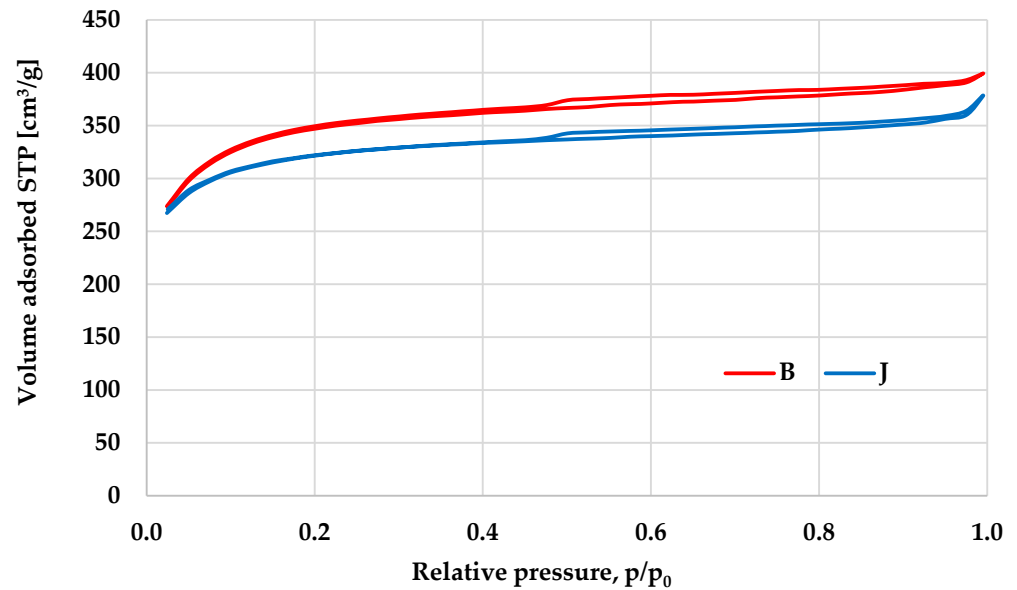
3. Results and Discussion

3.1. Textural Parameters of the Carbonaceous Materials Recovered from Utilized Water Filters

As it is commonly known, the possibilities of practical applications of activated carbon are mainly conditioned by its textural parameters. Therefore, in the first stage of the study, the size of the specific surface area and the total pore volume of the carbonaceous materials were determined in order to estimate their potential usefulness as adsorbents of organic pollutants from the liquid phase. According to the data presented in Table 1 and in Figures 3 and 4, both activated carbon samples obtained from the utilized filter cartridges have a well-developed surface area and a porous structure with a dominant number of micropores, which means that they have not lost their favourable textural parameters and can be used for adsorption purposes. The activated carbon recovered from the bottle filter (B) has a slightly larger surface area and, simultaneously, a greater total pore volume than the material recovered from the jug filter (J). The B sample also shows a slightly more microporous nature of the structure, as evidenced by both a greater proportion of micropores in the total pore volume as well as a smaller mean pore diameter.

Table 1. Textural parameters of the carbonaceous materials derived from the used carbon filters.

Sample	Surface Area [1] [m²/g]	Micropore Area [m²/g]	Total Pore Volume [cm³/g]	Micropore Volume [cm³/g]	Micropore Contribution [%]	Mean Pore Diameter [nm]
B	1042.58	998.26	0.619	0.540	87.2	2.376
J	957.67	921.12	0.586	0.498	84.9	2.451

[1] method error 2–5%.

Figure 3. N$_2$ adsorption-desorption isotherms of carbonaceous materials recovered from exhausted filter cartridges.
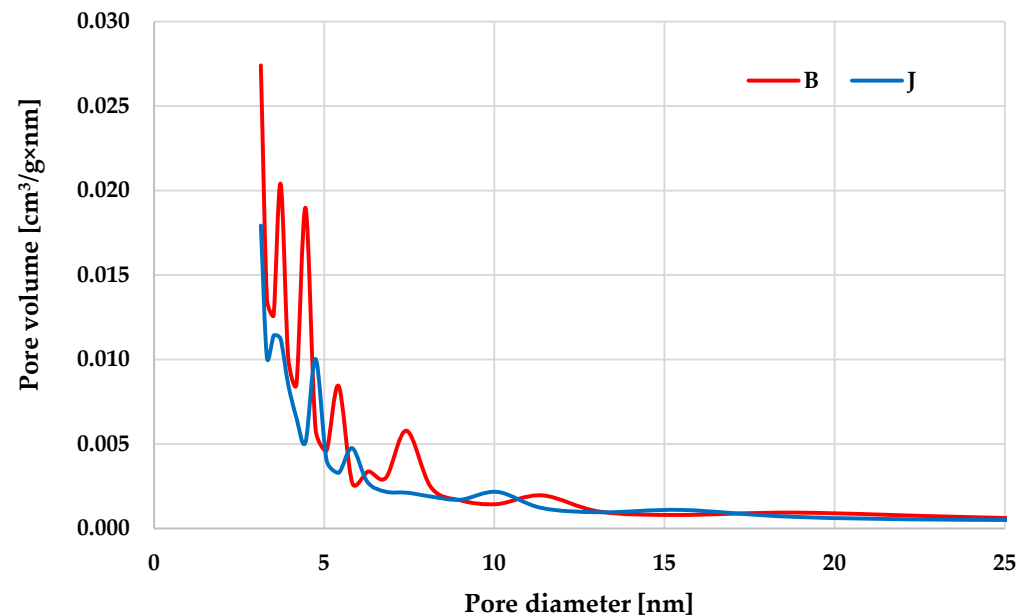
Figure 4. Pore size distribution of carbonaceous materials recovered from exhausted filter cartridges.

Significant micropores' contribution to the porous structure of the carbonaceous materials under investigation is also confirmed by the shape of the low-temperature N$_2$ sorption isotherms presented in Figure 3. According to the IUPAC classification, both isotherms are very similar to type I, which is characteristic of microporous or mesoporous

materials with pore sizes close to the micropore range. Moreover, for both activated carbon samples, a narrow hysteresis loop is observed, which indicates the presence of a certain amount of mesopores in their structures. Its shape is similar to the H4 type loop (acc. to IUPAC classification), which is characteristic of materials containing narrow slit-like pores. The presence of small mesopores in the structures of both carbon materials is also confirmed by the course of the pore size distribution curves presented in Figure 4. As seen, both samples have a great volume of pores with diameters within the range of 2–10 nm.

3.2. Acidic–Basic Properties of the Carbonaceous Materials Derived from the Used Carbon Filters

The chemical nature of the activated carbon surface and the share of mineral matter in its structure (which is just unnecessary ballast) are also very important from an adsorptive point of view. In order to fully characterize the acidic–basic properties of the activated carbon samples derived from the used carbon filters, the content of ash (mineral admixtures) as well as the surface functional group contribution were determined. Additionally, the pH value of their aqueous extracts was measured.

According to the data presented in Table 2, the carbonaceous materials differ quite significantly in terms of ash content and the acidic–basic character of the surface. Sample B, derived from a bottle filter, is characterized by a two-fold higher mineral substance contribution than activated carbon J, recovered from a jug filter. However, it should be emphasized that the ash content in both carbon materials is quite low, which is generally a desirable feature in the case of the adsorbents. The difference between the two carbonaceous materials may be a consequence of the diverse activation procedures used to produce the activated carbon. A variety of starting materials cannot be ruled out either. According to the declarations of the producers of both filters, the activated carbon included in their composition was obtained from coconut shells. However, it is well known that in the case of such precursors as biomass, the chemical structure is conditioned by the place of cultivation of a particular plant as well as the method of its fertilization. The construction of the filter and the way it is used by consumers are also very important.

Table 2. Mineral matter (ash) contribution as well as acidic–basic properties of the carbonaceous materials derived from the used carbon filters.

Sample	Ash Content [wt. %]	pH	Acidic Groups Content [mmol/g]	Basic Groups Content [mmol/g]
B	1.06	6.94	0.45	0.70
J	0.57	6.64	0.55	0.45

Further analysis of the data presented in Table 2 shows that the tested carbon materials are characterized by a diverse content of functional groups, both in terms of their quantity and type. Activated carbon derived from the bottle filter contains more functional groups on its surface, with a clear predominance of basic groups. The greater contribution of the functional groups of basic character may be to some extent a consequence of the higher ash content, which is usually alkaline in nature. In the case of the J sample, the content of functional groups is lower by 0.1 mmol/g, and acidic groups predominate on its surface. As a result, the pH value of its aqueous extract is slightly lower than that of sample B.

3.3. Sorption Performance of the Carbonaceous Materials Recovered from the Used Carbon Filters

In order to determine the sorption abilities of the activated carbon samples and to evaluate their usefulness for the removal of impurities from the liquid phase, three adsorbates of different molecular sizes were applied, i.e., iodine (I_2), methylene blue (MB), and malachite green (MG). According to the results presented in Figure 5, the carbonaceous materials derived from the exhausted carbon-based filters show very good sorption capacity towards all tested pollutants. In the case of I_2 adsorption, a more effective adsorbent turned out to be the activated carbon derived from a jug filter, which was able to adsorb 1326 mg of iodine from water. Alternatively, during the adsorption of both organic dyes from the liquid

phase, the activated carbon recovered from the bottle filter performed significantly better. It is particularly well seen in the case of MG adsorption, where the difference in sorption capacity of both carbonaceous materials is as much as 96.01 mg/g. For methylene blue, the observed difference is only 56.92 mg/g. This may be a consequence of the significantly larger molecular size of malachite green (Figure 2). These results are quite surprising because, according to the data presented in Table 1, sample J has a slightly larger mean pore diameter, which should favor the removal of adsorbates from larger molecules. However, in the case of the activated carbon recovered from the bottle filter, a significantly greater pore volume of sizes ranging from 2 to 10 nm is observed (Figure 4), which may facilitate MB and MG molecules' access to the inside part of the porous structure.
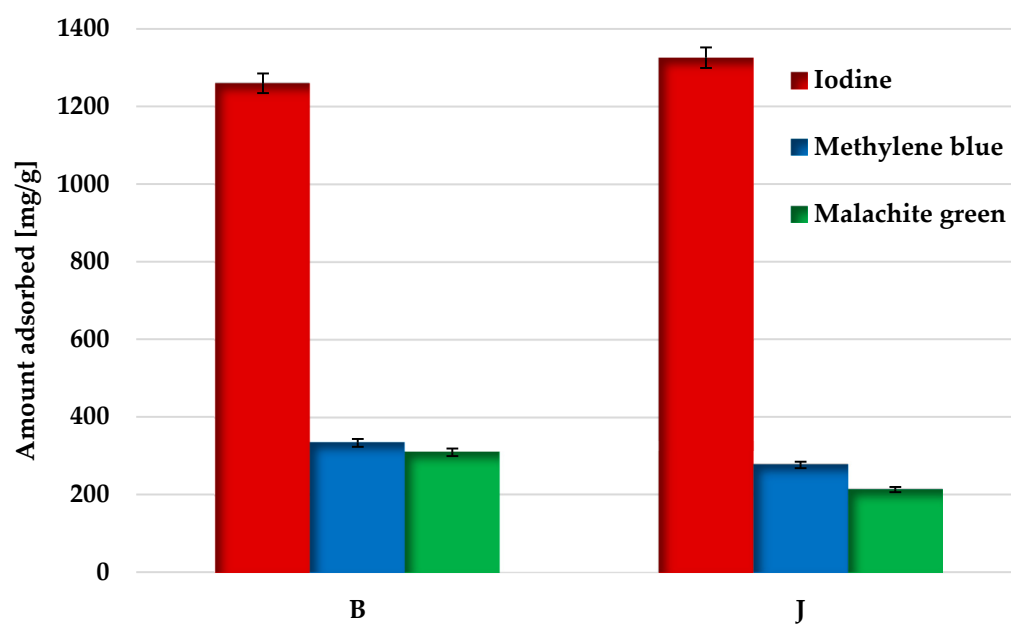
Figure 5. Adsorption capacity of carbonaceous materials towards iodine, methylene blue, and malachite green.

According to the data displayed in Figure 6, both carbonaceous materials derived from the exhausted filter cartridges show 100% efficiency in organic dye removal over a wide range of their initial concentrations. In the case of methylene blue adsorption, such a high efficiency is achieved in the range of 5–105 mg/dm^3 for the J sample and 5–120 mg/dm^3 for the B sample, respectively. Importantly, even at MB concentrations of the order of 150–175 mg/dm^3, the adsorption efficiency is very high and does not fall below 90%. In the case of malachite green adsorption, the situation is somewhat different. One-hundred percent efficiency of dye removal from the aqueous solution is reached in the range of 5–95 mg/dm^3 for the J sample and 5–140 mg/dm^3 for the B sample, respectively. However, a further increase in the initial concentration of this dye results in a rapid decrease in the effectiveness of its removal.

As follows from the analysis of the data presented in Figure 7, the amount of MB and MG adsorbed by the activated carbon samples increases significantly with increasing initial concentrations of the dye solutions, until a state of full saturation. It may indicate that at low concentrations, the adsorption of MB or MG takes place in a completely random way, which is caused by the availability of many free active sites on the surface/structure of the carbonaceous materials. At higher methylene blue or malachite green concentrations, all available active centers are occupied by dye molecules, and as a consequence, the complete saturation of the surface/porous structure of the tested carbon adsorbents is reached. Furthermore, the course of all the isotherms is smooth and single, which may suggest the monolayer coverage of the activated carbon surface with the methylene blue and malachite green molecules. This supposition is partially confirmed by the data collected

in Table 3, which present the parameters of the Langmuir and Freundlich model isotherms and describes MB and MG adsorption by the carbonaceous materials derived from the used carbon filters.
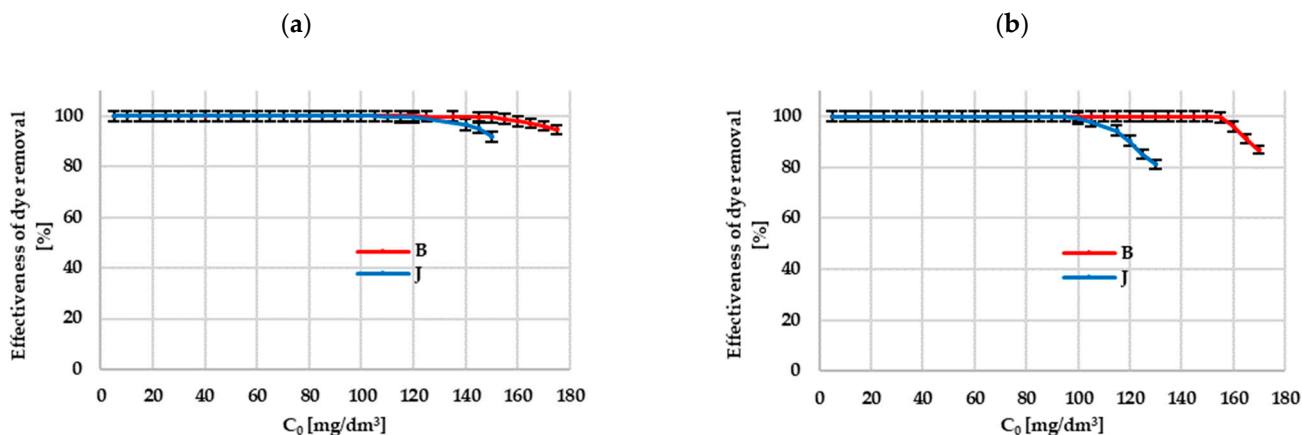
(**a**) (**b**)

Figure 6. The effectiveness of methylene blue (**a**) and malachite green (**b**) removal from the aqueous solutions.
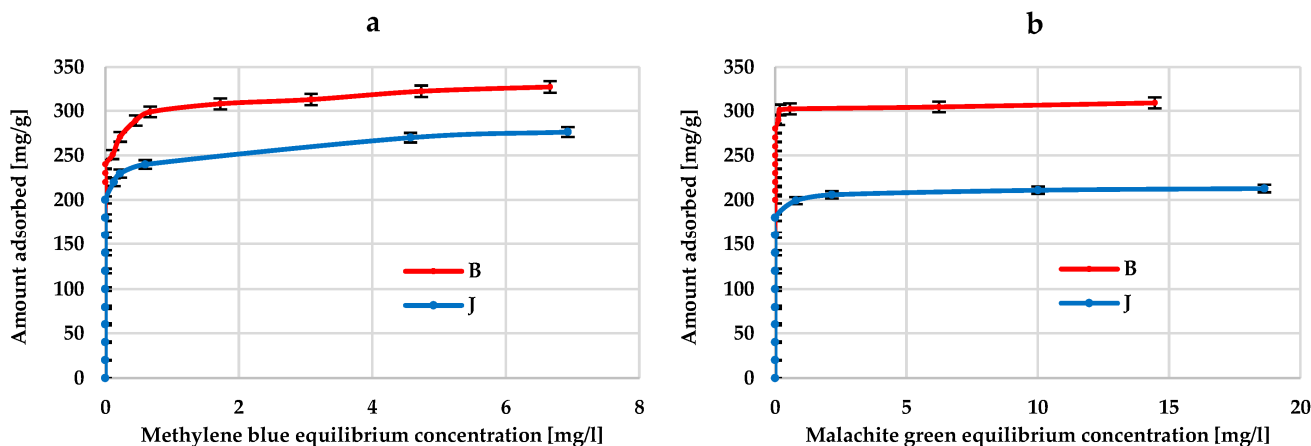
a b

Figure 7. The equilibrium isotherms of methylene blue (**a**) and malachite green (**b**) adsorption on the carbonaceous materials derived from the used carbon filters.

Table 3. Langmuir and Freundlich parameters of the isotherms of methylene blue and malachite green adsorption on the carbonaceous materials derived from the used carbon filters.

Sample	Langmuir Model			Freundlich Model		
	q_{max}	R^2	K_L	$1/n$	R^2	K_F
Methylene blue						
B	336.7	0.9994	0.11	0.057	0.9635	295.26
J	276.2	0.9999	0.43	0.053	0.9890	246.83
Malachite green						
B	308.64	0.9998	0.15	0.013	0.5633	304.43
J	215.98	0.9997	0.35	0.025	0.8725	200.91

q_{max}—the maximum adsorption capacity (mg/g), K_L—the Langmuir adsorption equilibrium constant (dm^3/mg), K_F—the Freundlich equilibrium constant [mg/g $(mg/dm^3)^{1/n}$], $1/n$—the intensity of adsorption, and R^2—the correlation coefficients.

According to these results, the Langmuir isotherm fits the experimental data more accurately than the Freundlich one. It is indicated by the significantly higher and very

close to unity values of the correlation coefficient R^2 for this model, especially in the case of the malachite green adsorption. Thus, it can be assumed that dye adsorption is most likely realized as the monolayer coverage of the activated carbon surface by the solute particles. However, in the case of methylene blue adsorption, the situation is not so obvious, in particular for the sample J, for which the R^2 value calculated for the Freundlich isotherm model is also very close to 1. This may suggest that the mechanism of the adsorbent-adsorbate interactions is more complex and involves multilayer adsorption.

As follows from the analysis of the data presented in Figure 8, the sorption capacity of the activated carbon samples toward both organic dyes decreases significantly with increasing temperature of the adsorbent-adsorbate system. This dependence is much more pronounced for sample B, derived from the bottle filter. In the case of methylene blue, the difference in the sorption capacity reached at temperatures of 25 and 35 °C is 18.90 mg/g, whereas in the case of malachite green, it is up to 30.25 mg/g. For the activated carbon derived from a jug filter, the differences are smaller and equal to 1.17 mg/g (for MB) and 20.32 mg/g (for MG), respectively. The decrease in the adsorption capacity with increasing temperature of the adsorbent-adsorbate system suggests that the reaction between the activated carbon and methylene blue or malachite green molecules is exothermic, and the adsorption is mainly based on a physical process that dominates at low temperatures. An increase in the temperature of the system can also lead to the weakening of bonds between the dye molecules and the active sites present on the adsorbent's surface, a consequence of which is the desorption process—some part of the MB or MG molecules is removed from the adsorbent's surface.
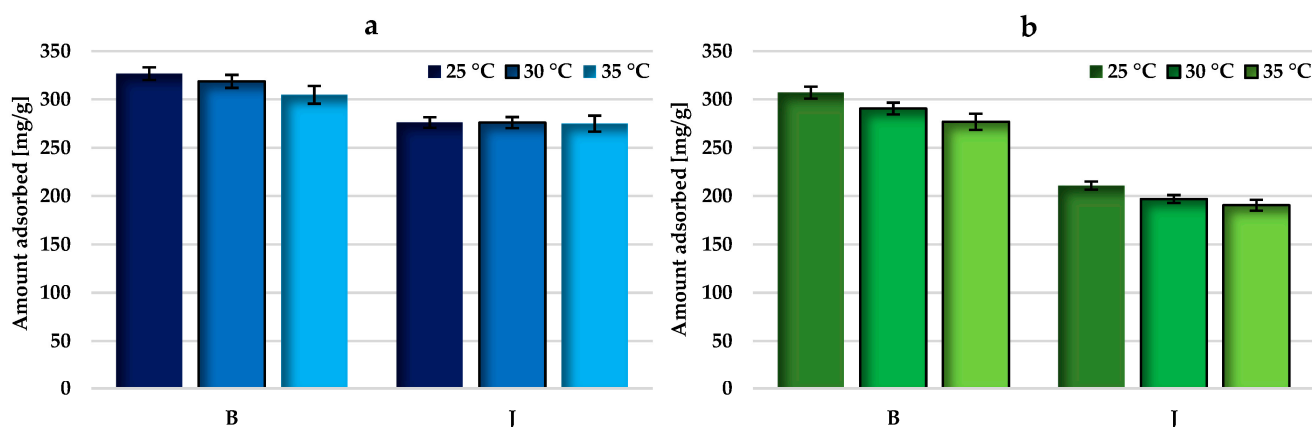
Figure 8. Effect of temperature on methylene blue (**a**) and malachite green (**b**) adsorption on the carbonaceous materials derived from the used carbon filters.

Another parameter that influences the efficiency of organic pollutant removal from aqueous solutions is pH. According to the data presented in Figure 9, the effect of this parameter is significant for both carbonaceous materials under investigation, especially in the case of malachite green adsorption. For the activated carbon derived from the bottle filter, the lowest adsorption capacity toward MB and MG was achieved at pH 6. The increase in pH results in an improvement in the removal efficiency of both dyes, reaching a maximum uptake at pH 12 and 10, respectively. In the case of malachite green, at pH 12, decomposition of the dye molecules took place. For the sample J derived from the jug filter, a similar tendency is observed, with the only difference being that the lowest adsorption capacity towards methylene blue was noted at pH 4. At lower pH values, surface functional groups present on the activated carbon surface are protonated, and the excess of H^+ ions can compete with the MB or MG molecules for the active sites, which can limit the adsorption of both dyes. At higher pH, as a consequence of surface group deprotonation, the concentration of H^+ ions significantly decreases and a negative charge appears at the activated carbon surface. This enables electrostatic attraction between the

molecules of cationic organic dyes and the negatively charged carbon surface and has a beneficial effect on the adsorption effectiveness.
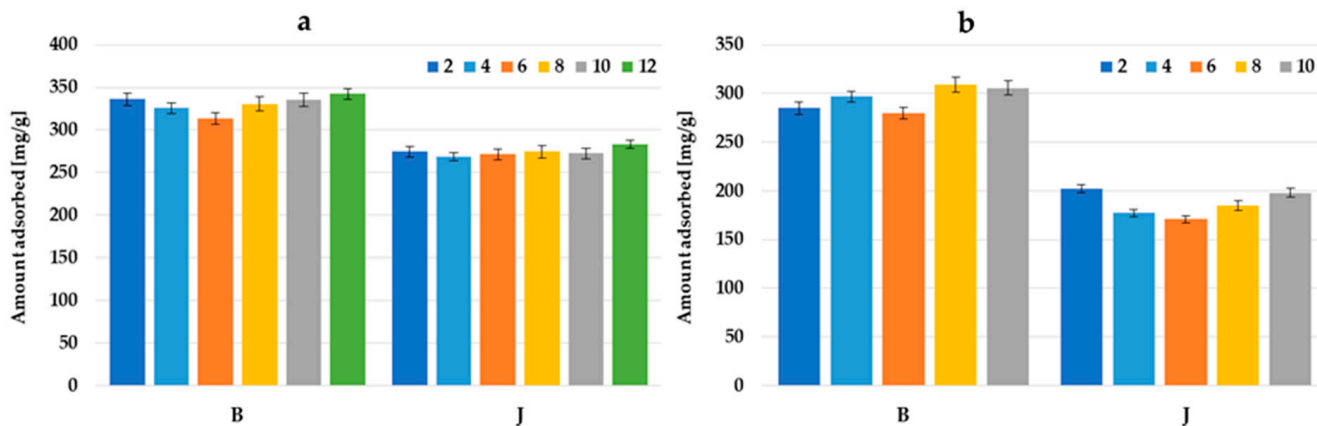
Figure 9. Effect of pH on methylene blue (**a**) and malachite green (**b**) adsorption on the carbonaceous materials derived from the used carbon filters.

The effect of contact time on methylene blue and malachite green adsorption on activated carbon samples derived from the used carbon filter is shown in Figure 10. According to these data, the kinetics of MB and MG adsorption consist of two stages: an initial rapid step, when adsorption is very fast and contributes significantly to equilibrium dye uptake, as well as a slower second phase, whose contribution to the total methylene blue or malachite green adsorption is considerably smaller. The first stage is most probably the instantaneous adsorption of MB and MG or the covering of the external activated carbon surface with adsorbate molecules. The second phase is the gradual dye adsorption that leads to equilibrium.
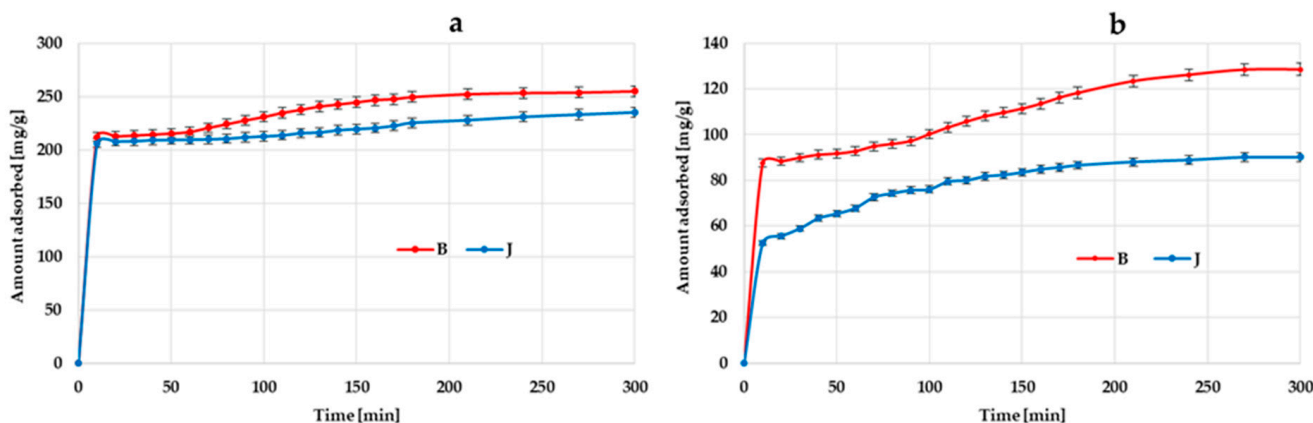
Figure 10. Effect of phase contact time on methylene blue (**a**) and malachite green (**b**) adsorption on the carbonaceous materials derived from the used carbon filters.

As follows from the analysis of the kinetics parameters collected in Table 4, the experimental data obtained for the sorption of methylene blue and malachite green on the activated carbon surface are better described by the kinetics equation of pseudo-second order. It is evidenced by the fact that the correlation coefficients of the linear regression for this model are close to 0.999, so they are significantly higher than the R^2 values obtained for pseudo-first order kinetic. PSO kinetics is also indicated by the fact that the values of q_{cal} are comparable to the experimentally determined ones (q_{exp}). It can also be supposed that the MB or MG adsorption involves mainly chemical interactions with the surface of the tested carbonaceous adsorbents.

Table 4. Kinetic parameters for MB and MG adsorption on the carbonaceous materials derived from the used carbon filters.

Sample	q_{exp}	PFO			PSO		
		q_{cal}	R^2	k_1	q_{cal}	R^2	k_2
Methylene blue							
B	254.74	82.71	0.9526	0.01497	263.15	0.9983	0.000395
J	235.03	44.68	0.9441	0.00875	238.09	0.9979	0.000573
Malachite green							
B	130.61	71.03	0.8963	0.010364	135.13	0.9879	0.000294
J	91.24	49.10	0.9871	0.012897	96.15	0.9977	0.000504

q_{exp}—experimental adsorption capacity [mg/g], q_{cal}—calculated adsorption capacity [mg/g], k_1—the pseudo-first order adsorption rate constant [1/min], k_2—the pseudo-second order adsorption rate constant [g/(mg·min)], R^2—correlation coefficients.

Based on the analysis of the data collected in Table 5, it can be concluded that activated carbon samples derived from the used filter cartridges perform very well in terms of iodine, methylene blue, and malachite green adsorption when compared to different carbonaceous adsorbents described in the literature. Therefore, they can be successfully applied in practice as the potential adsorbents of organic dyes from polluted water.

Table 5. Adsorption capacities towards iodine, methylene blue, and malachite green for various carbonaceous adsorbents.

Carbonaceous Adsorbent	Maximum Adsorbed Amount [mg/g]	Reference
Iodine		
Activated carbon from wastewater with high concentrations of organic matter	1800	[25]
Activated carbon from bean husks	1256	[26]
Activated carbon from miscanthus	1240	[27]
Activated carbon from mangosteen peel	1153	[28]
Activated biocarbon form mugwort	948	[29]
Activated carbon from used filters	1260 and 1326	This study
Methylene blue		
Activated carbon from wastewater with high concentrations of organic matter	240	[25]
Hydrochar from coffee husks	418	[30]
Activated carbon from bamboo chips	305	[31]
Activated carbon from rapeseed straw	250	[32]
Activated carbon from wood of *Paulownia tomentosa*	255	[33]
Activated carbon from used filters	276 and 333	This study
Malachite green		
Activated carbon from residue of supercritical extraction of marigold	622	[34]
Fe_3O_4@SiO_2–graphene oxides core–shell magnetic microspheres	265	[35]
Fe-BTC metal organic framework	177	[36]
Biowaste-derived carbon nanospheres	104	[37]
Cellulose nanofibril aerogels	213	[38]
Biochar derived from sheep manure	208	[39]
Activated carbon from used filters	212 and 308	This study

4. Conclusions

It has been shown that carbonaceous materials derived from used filter cartridges can be applied as alternative adsorbents of organic pollutants from aqueous solutions, which makes recycling them an excellent option. The activated carbon used as a component of water filter cartridges is able to effectively adsorb impurities of diverse molecule sizes.

More advantageous in this respect is the material derived from the bottle filter. Its sorption capacity towards iodine, methylene blue, and malachite green reaches levels of 1260 mg/g, 333.06 mg/g, and 308.75 mg/g, respectively. It has also been shown that the adsorption of coloured organic compounds proceeds in accordance with the mechanism proposed by Langmuir, i.e., with the formation of an adsorbate monolayer on the surface of the tested carbonaceous materials. The efficiency of the removal of cationic dyes from aqueous solutions is highest at a temperature of 25 °C, at pH 12 in the case of methylene blue, and at pH 10 for malachite green. As far as the kinetics of MB and MG adsorption are concerned, they were found to be best described by the pseudo-second order model.

Author Contributions: Conceptualization, P.N.; methodology, M.S. and P.N.; investigation, M.S.; resources, P.N.; data curation, P.N., writing—original draft preparation, M.S. and P.N.; writing—review and editing, M.S. and P.N.; visualization, M.S.; supervision, P.N. All authors have read and agreed to the published version of the manuscript.

Data Availability Statement: Data are contained within the article.

Conflicts of Interest: The authors declare no conflict of interest.

References

1. Mocek-Płóciniak, A.; Skowrońska, M. Water—An important element not only of the soil environment. *Soil Sci. Ann.* **2021**, *72*, 134620. [CrossRef]
2. Pavlidis, G.; Tsihrintzis, V.A. Environmental benefits and control of pollution to surface water and groundwater by agroforestry systems: A Review. *Water Resour. Manag.* **2018**, *32*, 1–29. [CrossRef]
3. Water Defense. Available online: https://waterdefense.org/water/contaminants/most-common-contaminants/ (accessed on 15 December 2022).
4. BRITA. Available online: https://www.brita.co.uk/ (accessed on 15 December 2022).
5. Çeçen, F.; Aktas, Ö. *Activated Carbon for Water and Wastewater Treatment: Integration of Adsorption and Biological Treatment*, 1st ed.; Wiley-VCH Verlag GmbH & Co. KGaA: Weinheim, Germany, 2011; pp. 13–41. [CrossRef]
6. Halicki, W.; Halicki, M. Effective removal of biogenic substances using natural treatment systems for wastewater for safer water reuse. *Water* **2022**, *14*, 3977. [CrossRef]
7. Wang, J.; Wang, R.; Ma, J.; Sun, Y. Study on the application of shell-activated carbon for the adsorption of dyes and antibiotics. *Water* **2022**, *14*, 3752. [CrossRef]
8. Wang, J.; Ma, J.; Sun, Y. Adsorption of methylene blue by coal-based activated carbon in high-salt wastewater. *Water* **2022**, *14*, 3576. [CrossRef]
9. Wiśniewska, M.; Pawlak, N.; Sternik, D.; Pietrzak, R.; Nowicki, P. Production of Activated Carbons from Food/Storage Waste. *Materials* **2023**, *16*, 1349. [CrossRef]
10. Jamal-Uddin, A.-T.; Matsuura, T.; Al-Daoud, F.; Zytner, R.G. Treatment and recycle of greenhouse nutrient feed water applying hydrochar and activated carbon followed by reverse osmosis. *Water* **2022**, *14*, 3573. [CrossRef]
11. Kayiwa, R.; Kasedde, H.; Lubwama, M.; Kirabira, J.B. active pharmaceutical ingredients sequestrated from water using novel mesoporous activated carbon optimally prepared from cassava peels. *Water* **2022**, *14*, 3371. [CrossRef]
12. Bazan-Wozniak, A.; Paluch, D.; Wolski, R.; Cielecka-Piontek, J.; Nosal-Wiercińska, A.; Pietrzak, R. Biocarbons obtained from fennel and caraway fruits as adsorbents of methyl red sodium salt from water system. *Materials* **2022**, *15*, 8177. [CrossRef]
13. Khan, S.; Ullah, R.; Adil, M.; Waheed, A.; Khan, K.A.; Ghramh, H.A.; Alharby, H.F.; Alzahrani, Y.M.; Alghamdi, S.A.; Alabdallah, N.M.; et al. Adsorption of pesticides using wood-derived biochar and granular activated carbon in a fixed-bed column system. *Water* **2022**, *14*, 2937. [CrossRef]
14. Kokkinos, E.; Lampou, A.; Kellartzis, I.; Karfaridis, D.; Zouboulis, A. Thiol-functionalization carbonaceous adsorbents for the removal of methyl-mercury from water in the ppb levels. *Water* **2022**, *14*, 49. [CrossRef]
15. Li, L.; Li, Y.; Liu, Y.; Ding, L.; Jin, X.; Lian, H.; Zheng, J. Preparation of a novel activated carbon from cassava sludge for the high-efficiency adsorption of hexavalent chromium in potable water: Adsorption performance and mechanism insight. *Water* **2021**, *13*, 3602. [CrossRef]
16. Gęca, M.; Wiśniewska, M.; Nowicki, P. Simultaneous removal of polymers with different ionic character from their mixed solutions using herb-based biochars and activated carbons. *Molecules* **2022**, *27*, 7557. [CrossRef]
17. Bazan-Wozniak, A.; Cielecka-Piontek, J.; Nosal-Wiercińska, A.; Pietrzak, R. Adsorption of organic compounds on adsorbents obtained with the use of microwave heating. *Materials* **2022**, *15*, 5664. [CrossRef]
18. Kazmierczak-Razna, J.; Zioła-Frankowska, A.; Nowicki, P.; Frankowski, M.; Wolski, R.; Pietrzak, R. Removal of heavy metal ions from one- and two-component solutions via adsorption on n-doped activated carbon. *Materials* **2021**, *14*, 7045. [CrossRef] [PubMed]

19. Regeneration/Active Carbon. Available online: https://www.lenntech.com/library/adsorption/regeneration/activecarbon-regeneration.htm (accessed on 3 February 2023).

20. Bazan-Wozniak, A.; Nowicki, P.; Pietrzak, R. The effect of demineralization on the physicochemical and sorption properties of activated bio-carbons. *Adsorption* **2019**, *25*, 337–343. [CrossRef]

21. Bazan-Wozniak, A.; Nowicki, P.; Wolski, R.; Pietrzak, R. Activated bio-carbons prepared from the residue of supercritical extraction of raw plants and their application for removal of nitrogen dioxide and hydrogen sulfide from the gas phase. *Materials* **2021**, *14*, 3192. [CrossRef]

22. Foo, K.Y.; Hameed, B.H. Insights into the modelling of adsorption isotherm systems. *Chem. Eng. J.* **2010**, *156*, 2–10. [CrossRef]

23. Marković, D.D.; Lekić, B.M.; Rajaković-Ognjanović, V.N.; Onjia, A.E.; Rajaković, L.V. A new approach in regression analysis for modelling adsorption isotherms. *Sci. World J.* **2014**, *2014*, 930879. [CrossRef]

24. Simonin, J.P. On the comparison of pseudo-first order and pseudo-second order rate laws in the modeling of adsorption kinetics. *Chem. Eng. J.* **2016**, *300*, 254–263. [CrossRef]

25. Hu, X.; Kong, L.; Zhu, F.; Peng, X. The recycling of acid wastewater with high concentrations of organic matter: Recovery of H_2SO_4 and preparation of activated carbon. *Water* **2022**, *14*, 183. [CrossRef]

26. Evwierhoma, E.T.; Madubiko, O.D.; Jaiyeola, A. Preparation and characterization of activated carbon from bean husk. *Niger. J. Technol.* **2018**, *37*, 674–678. [CrossRef]

27. Doczekalska, B.; Bartkowiak, M.; Waliszewska, B.; Orszulak, G.; Cerazy-Waliszewska, J.; Pniewski, T. Characterization of chemically activated carbons prepared from miscanthus and switchgrass biomass. *Materials* **2020**, *13*, 1654. [CrossRef]

28. Hanami, Z.A.; Lestari, P. Characterization and application of mangosteen peel activated carbon for ammonia gas removal. *Environ. Nat. Resour. J.* **2021**, *19*, 320–329. [CrossRef]

29. Wiśniewska, M.; Rejer, K.; Pietrzak, R.; Nowicki, P. Biochars and activated biocarbons prepared via conventional pyrolysis and chemical or physical activation of mugwort herb as potential adsorbents and renewable fuels. *Molecules* **2022**, *27*, 8597. [CrossRef]

30. Tran, T.H.; Le, A.H.; Pham, T.H.; Nguyen, D.T.; Chang, S.W.; Chung, W.J.; Nguyen, D.D. Adsorption isotherms and kinetic modeling of methylene blue dye onto a carbonaceous hydrochar adsorbent derived from coffee husk waste. *Sci. Total Environ.* **2020**, *725*, 138325. [CrossRef]

31. Jawad, A.H.; Abdulhameed, A.S. Statistical modeling of methylene blue dye adsorption by high surface area mesoporous activated carbon from bamboo chip using KOH-assisted thermal activation. *Energy Ecol. Environ.* **2020**, *5*, 456–469. [CrossRef]

32. Chen, J.; Tang, C.; Li, X.; Sun, J.; Liu, Y.; Huang, W.; Wang, A.; Lu, Y. Preparation and modification of rape straw biochar and its adsorption characteristics for methylene blue in water. *Water* **2022**, *14*, 3761. [CrossRef]

33. Alam, S.; Khan, M.S.; Bibi, W.; Zekker, I.; Burlakovs, J.; Ghangrekar, M.M.; Bhowmick, G.D.; Kallistova, A.; Pimenov, N.; Zahoor, M. Preparation of activated carbon from the wood of *Paulownia tomentosa* as an efficient adsorbent for the removal of Acid Red 4 and methylene blue present in wastewater. *Water* **2021**, *13*, 1453. [CrossRef]

34. Bazan-Wozniak, A.; Wolski, R.; Paluch, D.; Nowicki, P.; Pietrzak, R. Removal of organic dyes from aqueous solutions by activated carbons prepared from residue of supercritical extraction of marigold. *Materials* **2022**, *15*, 3655. [CrossRef] [PubMed]

35. Zhang, J.; Liu, M.; Liu, Z.; Yang, T.; He, Q.; Yang, K.; Wang, H. Studies of malachite green adsorption on covalently functionalized Fe_3O_4@SiO_2–graphene oxides core–shell magnetic microspheres. *J. Sol.-Gel. Sci. Technol.* **2017**, *82*, 424–431. [CrossRef]

36. Delpiano, G.R.; Tocco, D.; Medda, L.; Magner, E.; Salis, A. Adsorption of malachite green and alizarin red s dyes using Fe-BTC metal organic framework as adsorbent. *Int. J. Mol. Sci.* **2021**, *22*, 788. [CrossRef] [PubMed]

37. Krishnappa, B.; Bhat, V.S.; Ancy, V.; Joshi, J.C.; S, J.M.; Naik, M.; Hegde, G. Biowaste-derived, highly efficient, reusable carbon nanospheres for speedy removal of organic dyes from aqueous solutions. *Molecules* **2022**, *27*, 7017. [CrossRef] [PubMed]

38. Jiang, F.; Dinh, D.M.; Hsieh, Y.-L. Adsorption and desorption of cationic malachite green dye on cellulose nanofibril aerogels. *Carbohydr. Polym.* **2017**, *173*, 286–294. [CrossRef] [PubMed]

39. Dilekoğlu, M.F. Malachite green adsorption from aqueous solutions onto biochar derived from sheep manure: Adsorption kinetics, isotherm, thermodynamic, and mechanism. *Int. J. Phytoremediat.* **2022**, *24*, 436–446. [CrossRef]